Application of nanostructured ZnO films for electrochemical DNA biosensor

Maumita Das [a], Gajjala Sumana [a], R. Nagarajan [b], B.D. Malhotra [a,*]

[a] Department of Science and Technology Centre on Biomolecular Electronics, Biomedical Instrumentation Section, Materials Physics and Engineering Division, National Physical Laboratory (Council of Scientific and Industrial Research), Dr.K.S.Krishnan Marg, New Delhi 110012, India
[b] Department of Chemistry, University of Delhi, Delhi-110007, India

Keywords:
Zinc oxide (ZnO)
DNA biosensor
Electrochemical deposition

A B S T R A C T

Nanostructured zinc oxide (nsZnO) films have been fabricated onto conducting indium–tin–oxide (ITO) coated glass plate, by cathodic electro-deposition to immobilize probe DNA specific to *M. tuberculosis* via physisorption based on strong electrostatic interactions between positively charged ZnO (isoelectric point = 9.5) and negatively charged DNA to detect its complementary target. Electrochemical studies reveal that the presence of nano-structured ZnO results in increased electro-active surface area for loading of DNA molecules. The DNA–nsZnO/ITO bioelectrode exhibits interesting characteristics such as detection range of $1\times10^{-6}-1\times10^{-12}$ M, detection limit of 1×10^{-12} M (complementary target) and 1×10^{-13} M (genomic DNA), reusability of about 10 times, response time of 60s and stability of up to 4 months when kept at 4°C.

1. Introduction

Tuberculosis is world's leading chronic pulmonary bacterial infectious disease that kills millions of people each year. The disease is caused by the bacteria *Mycobacterium tuberculosis*, which mainly attacks lungs and is spread when an infected person coughs, sneezes or spits. Symptoms of the disease include chronic coughs with blood in the sputum, fever, night sweats and weight loss. The causative agent, *M. tuberculosis*, has a distinctive life cycle spanning different environments and developmental stages [1–4]. Although tuberculosis is a curable disease that responds well to antibiotics, it has re-emerged as a growing global health problem because of the development of drug-resistant strains. The resurgence of TB and increased risk for TB in HIV-infected persons has magnified the need for rapid, inexpensive and accurate methods for the diagnosis of TB [5]. Most widely used conventional techniques for detection of *M. tuberculosis*, such as PCR (polymerase chain reaction), RFLP (restriction fragment length polymorphism), immunoassays and southern hybridization, have high sensitivity and specificity but are known for their limitations in terms of labor intensiveness, increased assay time and high cost. Besides this, isolation, identification and drug susceptibility of testing of TB are major hazards in many laboratories, as it requires dedicated equipment and well-trained manpower [6].

Affinity biosensors have emerged a promising alternative for faster, cost-effective, and simpler methods of microbial detection using nucleic acids-based affinity detection of complementary target sequences. DNA biosensors based on guanine oxidation have recently been proposed for the detection of microbes. These DNA sensors utilize the interaction of DNA with various compounds either by monitoring changes in the DNA redox properties (i.e. guanine oxidation) or with an electro-active analyte intercalated on a DNA layer. Agustın Costa-Garcıa et.al. have developed enzymatic voltammetric immunosensor by simple adsorption and covalent immobilization techniques. The results indicate improved performance of this sensor using streptavidin as a coupler with detection limit of 1.0 ng/ml [7]. An electrochemical biosensor for the determination of short sequences from the *M. tuberculosis* (MTB) DNA has been reported by Joseph Wang et.al. The sensor relies on the modification of the carbon-paste transducer with 27- or 36-mer oligonucleotide probe and their hybridization to complementary strands from the MTB DNA. Chronopotentiometry is employed as transducer and the sensor has been reported to detect up to ng ml^{-1} level of the MTB DNA target [8]. Prabhakar et.al. have explored the cysteine modified NH_2-end peptide nucleic acid probe and 5′-thiol end labeled DNA probes immobilized onto BK-7 gold coated glass plates for specific detection of *M. tuberculosis* using SPR. Though, the sensor has high sensitivity and specificity, it has limitations in terms of high association time (8500 s), requirement of dedicated equipments, trained manpower and expensive reagents. PNA immobilized on polyvinyl sulfonate doped polypyrrole/ITO coated glass plates have also been utilized for tuberculosis detection using Ru complex and methylene blue indicator [9]. Relatively improved sensitivity with methylene blue indicator has been observed as compared to that of ruthenium complex due to its steric hindrance and creation of lesser number of charge carriers. Square wave voltammetry based DNA–PANI/Au and PNA–PANI/Au has also been utilized for the fabrication of DNA sensor. The sensor is reported to

* Corresponding author.
E-mail address: bansi.malhotra@gmail.com (B.D. Malhotra).

have improved repeatability (13–15 times). The sensor suffers from limitations like carcinogenicity, non-biocompatibility and non-reproducibility. The reported characteristics obviate the need for fabrication of cheaper, biocompatible and sensitive biosensor for detection of pathogenic diseases [10].

Nanostructured transparent metal oxides are known to have unique ability to promote faster electron transfer kinetics between electrode and the active site of desired enzyme [11]. Among the metal oxide nanoparticles, nanostructured zinc oxide (ZnO) attained technological importance for biosensors, smart windows and dye-sensitized solar cells etc because of their properties including high surface area, catalytic efficiency, isoelectric point ~ 9.5 and strong adsorption ability [12-16]. The high isoelectric point (IEP) of ZnO results in unique property to immobilize DNA having low isoelectric point through electrostatic interaction. Furthermore, nontoxicity, high chemical stability, and high electron transfer capability make ZnO as a promising material for immobilization of biomolecule and can be employed for developing implantable biosensors [17–21].

Therefore, in the present study, probe DNA immobilized on electrochemically deposited ZnO film (DNA–nsZnO/ITO) is explored for the detection of M.TB using methylene blue (MB) as redox intercalator.

2. Experimental details

2.1. Materials

Zinc chloride ($ZnCl_2$), Potassium chloride (KCl) and probe and complementary oligonucleotide sequence specific to *M. tuberculosis* were procured from Sigma-Aldrich, India. Indium–tin–oxide (ITO) coated glass plates were obtained from Balzers, UK. All the chemicals and reagents used in the present studies were of molecular biology (MB) grade. These reagents were prepared in de-ionized water (Milli Q 10 TS). All the solutions and glassware were autoclaved prior to being used.

Probe sequence: 5′-GGT CTT CGT GGC CGG CGT TCA-3′
Complementary sequence (target): 5′-TGA ACG CCG GCC ACG AAG ACC-3′
One-base mismatch: 5′-TGA-ACG-CCG-ACC-ACG-AAG-ACC-3′
Non-complementary: 5′-ATG-TCT-CAA-GCC-AGC-TGC-TG-3′

2.2. Electrochemical deposition of nanostructured zinc oxide film on ITO (nsZnO/ITO) coated glass plates

The electro-deposition of nanostructured ZnO films have been carried out from an aqueous electrolyte containing of 8 mM zinc chloride and 0.1 M potassium chloride by applying a constant cathodic potential of −1.0 V to −1.4 V for different deposition times between 5 and 15 min at 70–80 °C in a water bath, using an electrochemical cell containing Ag/AgCl as reference electrode, platinum wire as counter electrode and ITO as working electrode (0.25 cm^2) using Potentiostat/Galvanostat.

2.3. Immobilization of probe DNA (ssDNA) onto nsZnO/ITO electrode

Oligonucleotide probe containing 21 bases, specific to *M. tuberculosis*, has been immobilized onto nsZnO/ITO film in a humid chamber at 25 °C using electrostatic interactions between the positively charged ZnO (IEP = 9.5) and the negatively charged DNA (IEP ~ 4).

2.4. Characterization

The X-ray diffraction technique (XRD) and Fourier transform infrared (FT-IR) spectra have been recorded on X-ray diffractometer (Miniflex II Desktop, Rigaku Company) and Perkin Elmer instrument, Model Spectrum BX II respectively. The morphological studies are performed with scanning electron microscope (LEO-40). Potentiostat/Galvanostat (Autolab Eco Chemie, Netherlands) is used for electrochemical measurements as well as electrochemical impedance spectroscopy measurements (0.01–10^5 Hz). These measurements are carried out using a three electrode cell with DNA–nsZnO/ITO bioelectrode as the working electrode, platinum (Pt) wire as the counter electrode, and saturated Ag/AgCl electrode as a reference electrode in phosphate buffer saline [PBS (50 mM, pH 7.0, 0.9% NaCl)] containing [$Fe(CN)_6^{-3/-4}$] (5 mM).

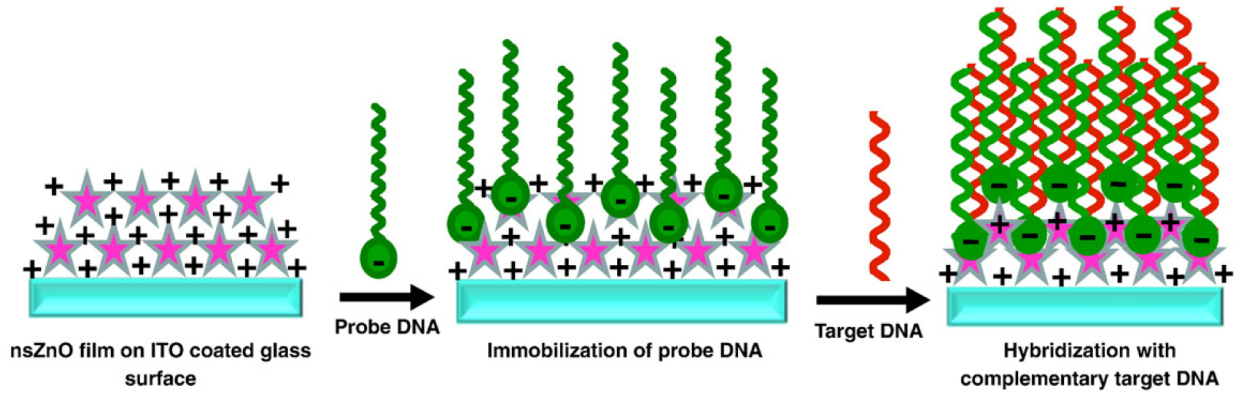

Schematic of DNA immobilization onto nsZnO film and hybridization with target sequence.

3. Results and discussion

3.1. Optical properties

Fig. 1A shows the X-ray diffraction patterns obtained for electrochemically deposited ZnO film, recorded using CuKα radiation from 20°to 80°(2 theta). The diffraction pattern shows three peaks of (100), (002) and (200) orientation planes with different intensities. This reveals that grains of zinc oxide grow along different directions. All these peaks with broad humps are attributed to the diffraction lines pertaining to nano sized zinc oxide having wurtzite structure. The crystallite size of this film is estimated as 27 nm using Scherer equation.

Fig. 1B shows the FT-IR spectra of nsZnO/ITO (curve a) and DNA–nsZnO/ITO (curve b) electrodes respectively. The presence of sharp and intense bands at 498 cm^{-1} and 680 cm^{-1} indicates the formation of ZnO film on ITO surface. In Fig. 1B (curve b), peaks at 1240, 1610 and 1760 cm^{-1} are due to the P–O and C–O stretching vibration of PO_4 backbone and purine and pyrimidine rings of DNA, respectively. The broad band at 3210 cm^{-1} is attributed to the N–H stretching vibration of the amide moiety.

SEM (Fig. 2A) studies of nsZnO/ITO film reveal that the size of the grain is regular with hexagonal morphology having particle size ranging from 50-100 nm without any cracks and voids. However, surface morphology of DNA–nsZnO/ITO electrode changes after the immobilization of DNA (Fig. 2B) revealing immobilization of DNA onto ns–zinc oxide film.

Fig. 2C and D shows the AFM pictures obtained for the ZnO and DNA–nsZnO films on ITO surface, respectively. Fig. 2C reveals the formation of rough microstructure having uniformly distributed nano pores. The formation of rough and porous microstructure is attributed to the electrochemical deposition of ZnO film. The roughness parameters for nsZnO/ITO surface (Fig. 2C) and for DNA–nsZnO/ITO (Fig. 2D) surface have been experimentally determined as 3.51 and 2.74 nm, respectively. It may be noted that the decreasing roughness in DNA–nsZnO/ITO surface arises due to the immobilization of DNA onto the porous ZnO film. The particle size of nsZnO film obtained from AFM study ranges from 30 to 100 nm.

3.2. Electrochemical studies

The biosensor has been characterized using electrochemical impedance spectroscopy (EIS). Fig. 3A shows EIS spectra of DNA–nsZnO/ITO electrode (curve a), ITO electrode (curve b) and nsZnO/ITO bioelectrodes (curve c) investigated in PBS (pH = 7.0, 0.9% NaCl) containing 0.05 M $[Fe(CN)_6]^{3-/4-}$ in the frequency range of 0.01–10^5 Hz. In the EIS, the semicircle part corresponds to electron transfer limited process and its diameter is equal to the electron transfer resistance, R_{et} that controls electron transfer kinetics of the redox probe at the electrode interface. The R_{et} values for (a) DNA–nsZnO/ITO, (b) bare ITO and (c) nsZnO/ITO electrodes are 1224 Ω, 2778 Ω, and 3357 Ω, respectively. The decrease in R_{et} can be assigned to potential generated in the open circuit and pH of buffer causing polarization of NH_2 group in DNA backbone resulting in positive charge on DNA–nsZnO/ITO surface [9]. This positive charge attracts negative charge of $[Fe(CN)_6]^{3-/4-}$ resulting in reduced charge transfer resistance from solution to surface. Further decrease in the R_{et} value from bare ITO to nsZnO/ITO is due to the conducting nature of the ITO compared to that of ZnO matrix. In cyclic voltammetry, there is a considerable sharp increase in the oxidation current (Fig.3B) from 1.46×10^{-4}A for nsZnO film (curve c) to 3.43×10^{-4} A for DNA-nsZnO film (curve a) that may be attributed to the guanine oxidation of randomly distributed DNA molecules on nsZnO film. The decrease in oxidation current in case of nsZnO/ITO compared to ITO (curve b) may be due the insulating nature of ZnO.

4. Electrochemical response studies

The electrochemical response of the DNA–nsZnO/ITO bioelectrode has been investigated as a function of complementary target DNA

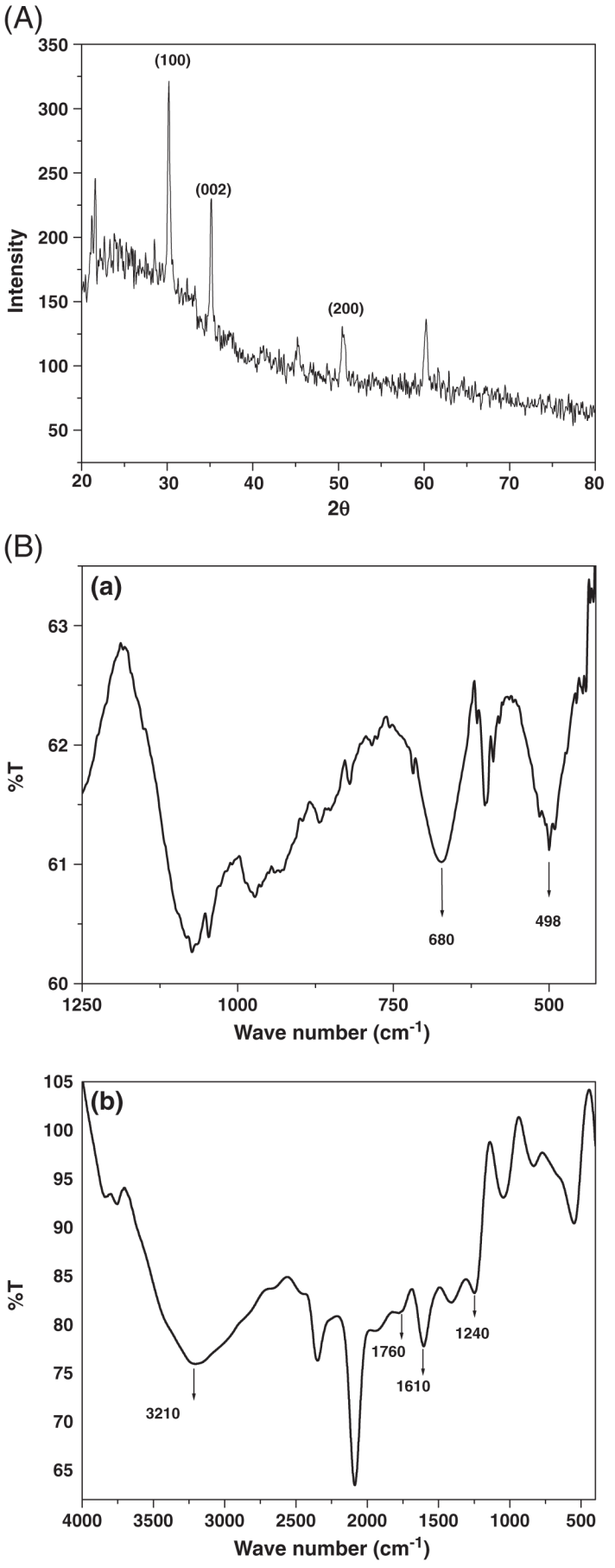

Fig. 1. (A) XRD pattern of nanostructured ZnO thin film and (B) FT-IR spectra of (a) nsZnO/ITO and (b) DNA–nsZnO/ITO film.

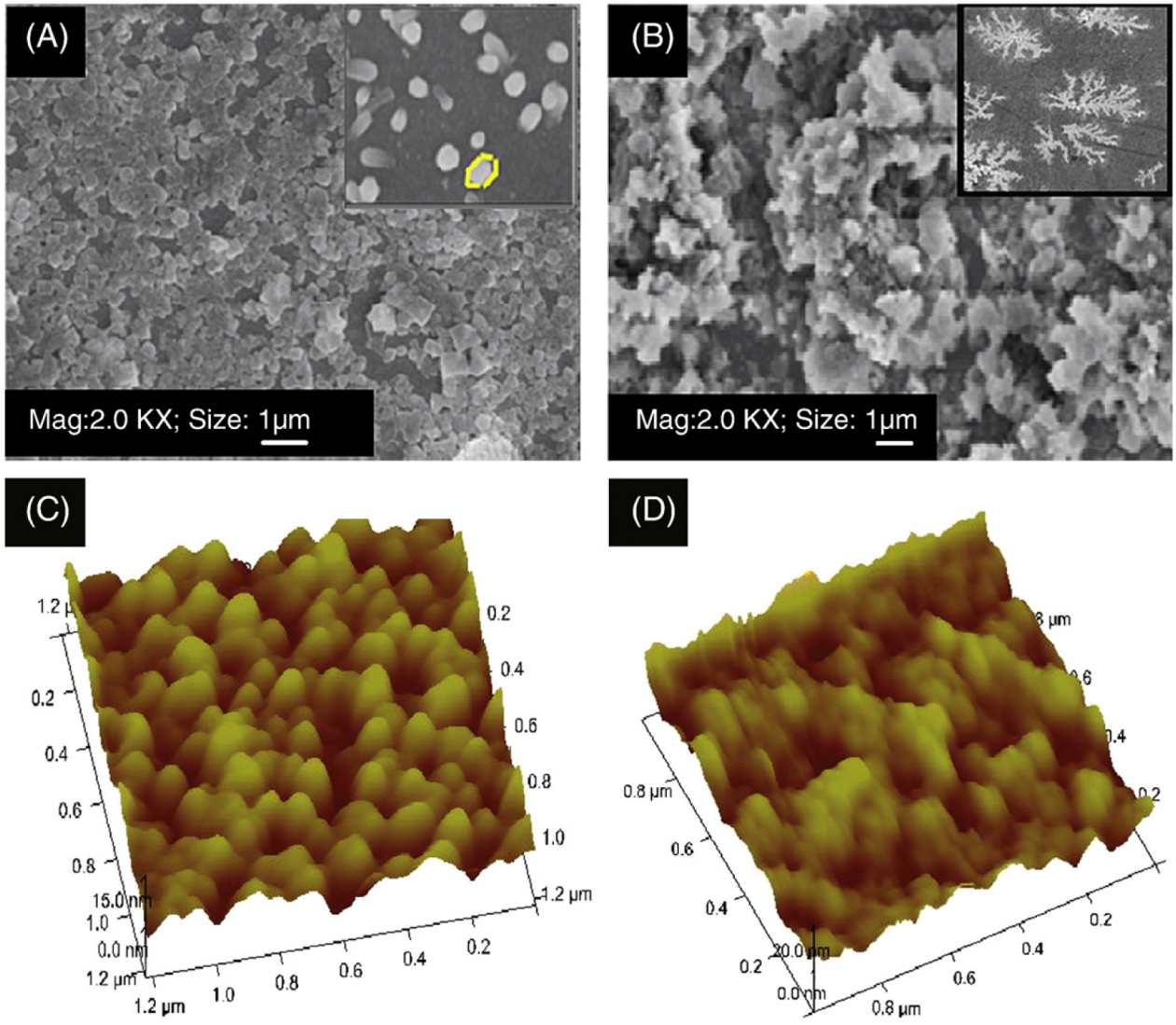

Fig. 2. SEM (A and B) and AFM images (C and D) of nsZnO/ITO and DNA–nsZnO/ITO electrodes.

concentration (1×10^{-6}–1×10^{-12} M) using methylene blue (MB) as hybridization indicator by differential pulse voltammetry (DPV) technique (Fig. 4A). The magnitude of current response is found to increase with decrease of target DNA concentration from 1×10^{-6} to 1×10^{-12}, revealing 1×10^{-12} as the detection limit. This decrease in the MB peak height with increase in the complementary DNA concentration may be attributed to the hindrance provided to MB–guanine interactions due to increased double stranded DNA formation. No further decrease in the MB signal above 1×10^{-6} is observed which reveals that all the hybridization sites on the DNA–nsZnO/ITO bioelectrodes are covered. The anodic peak current of MB has been found to be linear with the logarithmic value of the complementary oligonucleotides concentration and follows Eq. (1);

$$I_{complementary} = -1.43\times10^{-6}[\ln(\textit{target DNA concentration in M})] - 1.93\times10^{-7} \quad (1)$$

with regression coefficient (r^2) 0.99 and sensitivity of this bioelectrode is -1.43×10^{-6}.

The selectivity of this electrode has been investigated by monitoring the change in methylene blue oxidation current by incubating with complementary, non-complementary and one-base mismatch oligonucleotide sequence. Fig. 4B shows the DPV signal of MB at DNA–nsZnO/ITO electrode and after incubation with the same amount of complementary, non-complementary and one-base mismatch DNA sequence. The highest MB signal is obtained with the DNA probe on the ZnO/ITO electrode alone, because MB has a strong affinity for the free guanine bases and hence the greatest amount of MB accumulation occurs at this surface. A significant decrease in the signal of MB is observed when incubating with the complementary target sequence, which is because the interaction of MB and guanine moeties. The peak current value hardly decreases when the ssDNA–nsZnO/ITO electrode is exposed to the non-complementary oligonucleotide in the control experiments, which indicates that no change occurs at the electrode surface, and hence hybridization is not achieved. Negligible change after incubation with one-base mismatch sequence is observed indicating the selectivity of the bioelectrode for the hybridization detection.

Fig. 4C exhibits results of DPV studies of DNA–nsZnO/ITO bioelectrode on hybridization with heat-denatured *M. tuberculosis* genomic DNA. With increasing genomic DNA concentration (1×10^{-13} M–1×10^{-10} M), MB oxidation current ($I_{genomic}$) decreases, indicating increased number of DNA duplexes formed at the ZnO surface (Eq. (2)). The lower detection limit of ssDNA–nsZnO/ITO electrode with genomic DNA is found to be 1×10^{-13} M

$$I_{genomic\ DNA\ concentration} = -2.47\times10^{-5}[\ln(\textit{genomic DNA concentration in M})] - 4.24\times10^{-5} \quad (2)$$

with regression coefficient (r^2) = 0.85 Table 1 gives characteristics of this DNA biosensor along with those reported in literature.

3. Conclusions

Hexagonal ZnO nanocrystalline films (crystallite size ~ 27 nm and surface roughness 3.51 nm) have been electrochemically deposited

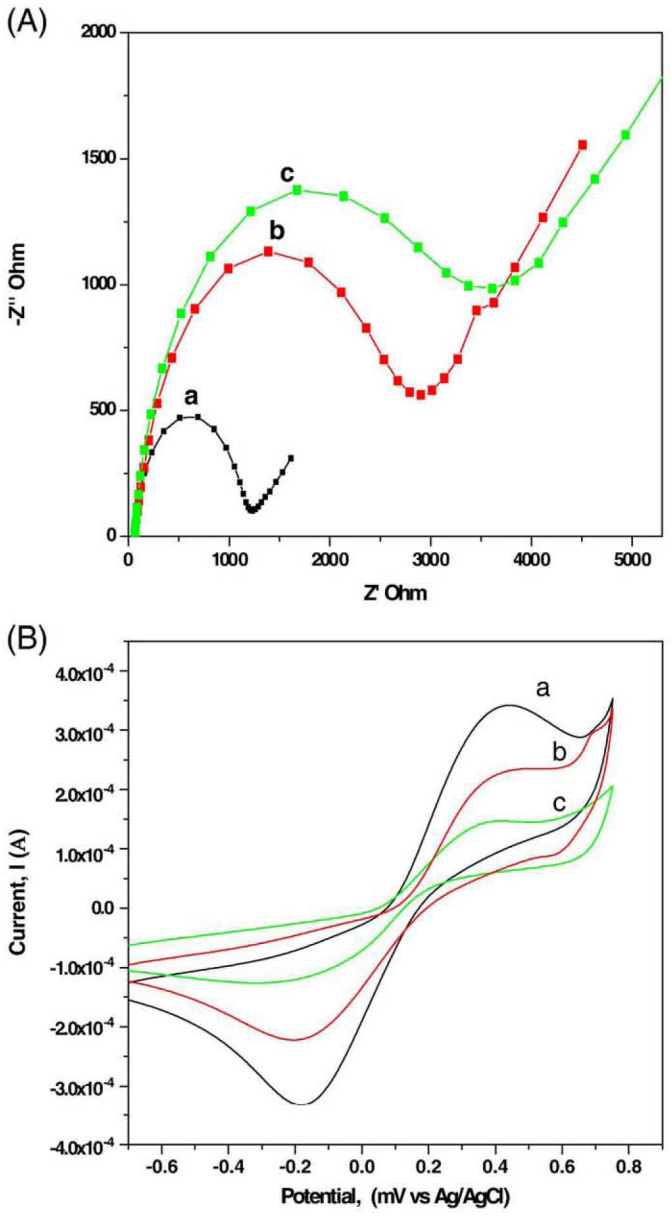

Fig. 3. Electrochemical impedance studies (A) and Cyclic votammogram (B) of (a) DNA–nsZnO/ITO, (b) ITO, (c) nsZnO/ITO electrodes in PBS solution (pH = 7.0, 0.9% NaCl) containing 0.05 M $[Fe(CN)_6]^{-3/4-}$.

onto ITO coated glass substrates from an aqueous electrolyte containing $ZnCl_2$ and KCl and have been utilized for the fabrication of DNA bioelectrode for detection of *M. tuberculosis.* DNA–nsZnO/ITO bioelectrode exhibits sensing characteristics such as detection range of 1×10^{-6} to 1×10^{-12} M, detection limit of 1×10^{-12} M, response time of 60 s and high sensitivity of 1.43×10^{-6}. Further, this bioelectrodes can detect genomic target DNA up to 1×10^{-13} M. Efforts should be made to use this bioelectrode with clinical samples and to fabricate DNA sensors for detection of *Pneumonia* and *cholera* etc.

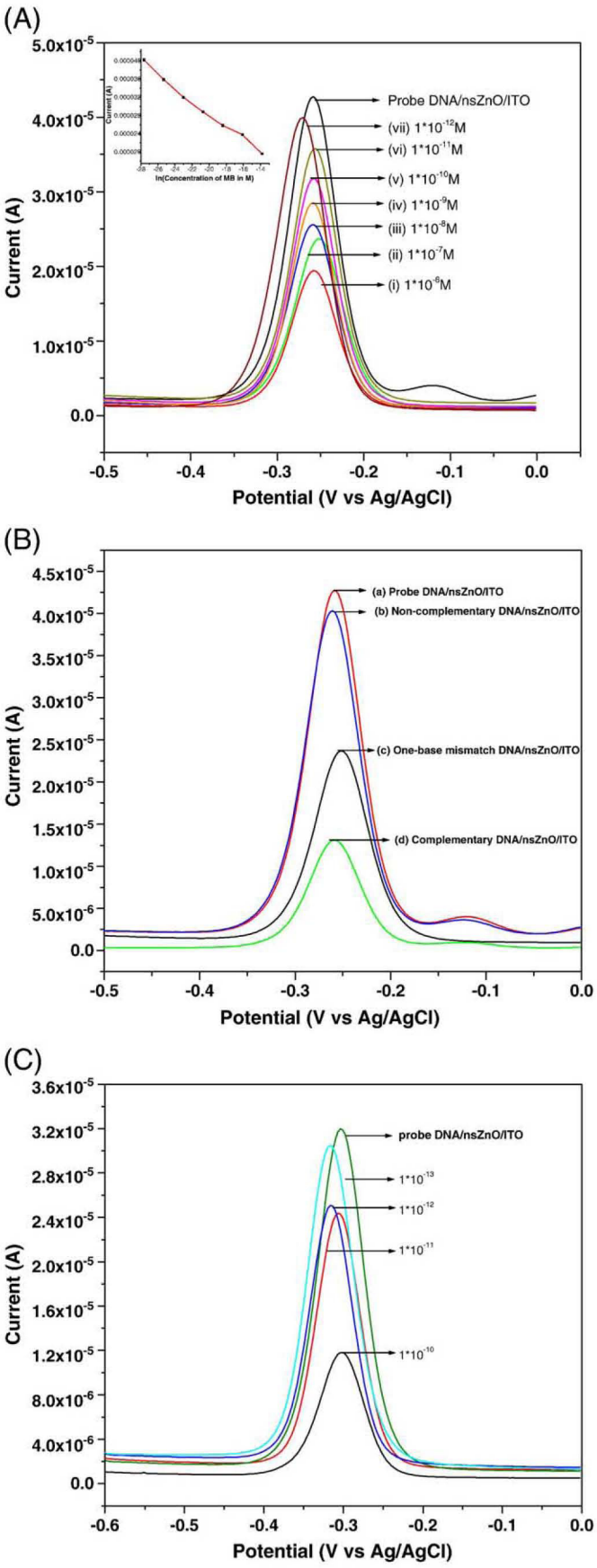

Fig. 4. (A) DPV studies of DNA-nsZnO/ITO electrode with respect to concentration of complementary target DNA sequence [inset shows the MB peak height as a function of ln(target DNA concentration)]; (B) Specificity studies of (a) probe DNA-nsZnO/ITO after incubation with (b) non-complementary, (c) one-base-mismatch, (d) complementary DNA sequence and (C) DPV studies of DNA-nsZnO/ITO electrode with respect to genomic DNA concentration in phosphate buffer (pH 7.0) containing 10 μM methylene blue.

Table 1
Characteristics of the various DNA biosensors used for *M. tuberculosis* detection.

Sl. no	Matrix	Biocompatibility	Reproducibility	Cross-linker/modifier used	Cost effectiveness	Stability	Reusability	Reference
1	Gold	Yes	–	Thiol	Expensive	–	–	6
2	Carbon	Yes	–	Avidin–biotin coupling	Cheap	4–5 weeks	–	7
3	Ppy-PVS	Yes	Poor	Pyrrole-2-carboxy aldehyde	Cheap	–	8 times	9
4	nsZnO/ITO	Yes	8 times	Not used	Cheap	>4 months	10 times	Present work

Acknowledgements

We thank Prof. R.C. Budhani, Director, National Physical Laboratory, India for the facilities. Maumita Das is thankful to CSIR, India for the award of a Senior Research Fellowship. The financial support received from Department of Science and Technology, India under the projects GAP 081132 and GAP 080232 is greatly acknowledged.

References

[1] M.C. Good, A.E. Greenstein, T.A. Young, H.L. Ng, T. Alber, J. Mol. Biol. 339 (2004) 459.
[2] A.L. Chun, Nat. Nanotechnol. 4 (2009) 698.
[3] D.G. Russell, Nature Rev. Mol. Cell. Biol. 2 (2001) 569.
[4] S.G. Reed, M.R. Alderson, W. Dalemans, Y. Lobet, Y.A. Skeiky, Tuberculosis (Edinb.) 83 (2003) 213.
[5] S.T. Thanyani, V. Roberts, D. Gilbert, R. Siko, P. Vrey, J.A. Verschoor, J. Immun. Methods 332 (2008) 61.
[6] N. Prabhakar, K. Arora, S.K. Arya, P.R. Solanki, M. Iwamoto, H. Singh, B.D. Malhotra, Analyst 133 (2008) 1587.
[7] M.D. Gonzalez, M.B.G. Garcıa, A.C. Garcıa, Biosens. Bioelectron. 20 (2005) 2035.
[8] J. Wang, G. Rivas, X. Cai, N. Dontha, H. Shiraishi, D. Luo, F.S. Valera, Anal. Chim. Acta 337 (1997) 41.
[9] N. Prabhakar, H. Singh, B.D. Malhotra, Electrochem. Commun. 10 (2008) 821.
[10] N. Prabhakar, K. Arora, H. Singh, B.D. Malhotra, J. Phys. Chem. B 112 (2008) 4808.
[11] M. Das, G. Sumana, R. Nagarajan, B.D. Malhotra, Appl.Phys.Lett. 96 (2010) 133703.
[12] H. Zhou, X. Gan, J. Wang, X. Zhu, G. Li, Anal. Chem. 77 (2005) 6102.
[13] S.A. Kumar, S.M. Chen, Anal. Lett. 41 (2008) 141.
[14] S.P. Singh, S.K. Arya, M.K. Pandey, B.D. Malhotra, S. Saha, K. Sreenivas, V. Gupta, Appl. Phys. Lett. 91 (2007) 063901.
[15] A. Wei, X.W. Sun, J.X. Wang, Y. Lei, X.P. Cai, C.M. Li, Z.L. Dong, W. Huang, Appl. Phys. Lett. 99 (2006) 123902.
[16] J.X. Wang, X.W. Sun, A. Wei, Y. Lei, X.P. Cai, C.M. Li, Z.L. Dong, Appl. Phys. Lett. 88 (2006) 233106.
[17] X. Zhu, I. Yuri, X. Gan, I. Suzuki, G. Li, Biosens. Bioelectron. 8 (2007) 1600.
[18] Z.Y. Fan, J.G. Lu, Appl. Phys. Lett. 86 (2005) 123510.
[19] C.X. Xu, X.W. Sun, C.B. Yuen, J. Chen, S.F. Yu, Z.L. Dong, Appl. Phys. Lett. 86 (2005) 011118.
[20] S. Kumar, V. Gupta, K. Sreenivas, Nanotechnology 16 (2006) 1167.
[21] J.X. Wang, X.W. Sun, A. Wei, Y. Lei, X.P. Cai, C.M. Li, Z.L. Dong, Appl. Phys. Lett. 88 (2006) 233106.